The Role of the Laser Pulse Duration in Infrared Matrix-Assisted Laser Desorption/Ionization Mass Spectrometry

Christoph Menzel,* Klaus Dreisewerd, Stefan Berkenkamp, and Franz Hillenkamp
Institute of Medical Physics and Biophysics, University of Muenster, Muenster, Germany

The role of the laser pulse duration in matrix-assisted laser desorption/ionization mass spectrometry with infrared lasers (IR-MALDI-MS) emitting in the 3 μm wavelength range has been evaluated. Mass spectrometric performance and characteristics of the IR-MALDI process were examined by comparing a wavelength-tuneable mid-infrared optical parametric oscillator (OPO) laser of 6 ns pulse duration, tuned to wavelengths of 2.79 and 2.94 μm, with an Er:YAG laser (λ = 2.94 μm) with two pulse durations of 100 and 185 ns, and an Er:YSGG laser (λ = 2.79 μm) with a pulse duration of 75 ns. Threshold fluences for the desorption of cytochrome *C* ions were determined as a function of the laser pulse duration for various common IR-MALDI matrices. For the majority of these matrices a reduction in threshold fluence by a factor of 1.2–1.9 was found by going from the 75–100 ns long pulses of the Erbium lasers to the short 6 ns OPO pulse. Within the experimental accuracy threshold fluences were equal for the 100 and the 185 ns pulse duration of the Er:YAG laser. Some pronounced pulse duration effects related to the ion formation from a glycerol matrix were also observed. The effect of the laser pulse length on the duration of ion emission was furthermore investigated. (J Am Soc Mass Spectrom 2002, 13, 975–984) © 2002 American Society for Mass Spectrometry

Matrix-assisted laser desorption/ionization mass spectrometry (MALDI-MS) [1] has become a major analytical method for the analysis of macromolecular compounds. In the great majority of cases lasers emitting in the ultraviolet (UV) with wavelengths between 266 to 355 nm and pulse durations between 0.5 and about 20 ns are used for MALDI. Energy deposition in this wavelength range is based on the strong electronic absorption of the aromatic matrix compounds. In contrast, in MALDI-MS with infrared lasers (IR-MALDI) the energy deposition takes place via vibrational excitation of functional groups of the matrices. Around 3 μm wavelength, typically the O–H and N–H stretch vibrations and around 10 μm the C–O stretch or O–H bending vibrations are IR active [2, 3].

A low extent of metastable fragmentation compared to its UV-MALDI counterpart was reported for IR-MALDI in various studies [4–9]—which can in particular be of advantage for the analysis of very labile biomolecules like large nucleic acids [8]. Lasers with different temporal profiles have been employed successfully for IR-MALDI-MS. Most commonly, erbium solid state lasers like the Erbium Yttrium-Aluminum-Garnet laser (Er:YAG) or the Erbium Yttrium-Scandium-Gallium-Garnet laser (Er:YSGG) emitting at wavelengths of 2.94 [2] and 2.79 μm [4], respectively, or transversely excited atmospheric pressure carbon dioxide lasers (TEA-CO_2) with emission wavelengths around 10 μm [3, 9] are used as IR-MALDI laser sources.

Whereas these laser systems typically exhibit pulse durations in the range of 60–200 ns, the more recently employed optical parametric oscillator (OPO) lasers have significantly shorter pulse durations of typically 5–10 ns [6, 10–14], determined by the pump laser of the system. In a number of fundamental studies on IR-MALDI the wavelength-tuneable Vanderbilt free-electron laser (FEL) with a different pulse profile was also used [15–17]. This laser emits "macropulses" of a few microseconds which actually consist of μs-long trains of ca. 1 ps-long micropulses separated in time by approximately 350 ps. For IR-MALDI, typically 100 ns-long pulses are switched-out from the FEL macropulse by means of an electro-optical Pockels cell. Pulse trains of up to several microseconds in duration have however also been tested [16, 18]. With this laser Cramer et al. found a quite strong dependence of the threshold fluence as well as of the temporal signal widths on the

Published online June 25, 2002

Address reprint requests to Dr. F. Hillenkamp, Institute of Medical Physics and Biophysics, University of Muenster, Robert-Koch Str. 31, D-48149 Muenster, Germany. E-mail: hillenk@uni-muenster.de

*Current address: Geneprot, Inc., Pré de la Fontaine 2, CH-1217 Meyrin, Switzerland.

© 2002 American Society for Mass Spectrometry. Published by Elsevier Science Inc.
1044-0305/02/$20.00
PII S1044-0305(02)00397-5

Received January 29, 2002
Revised March 21, 2002
Accepted March 29, 2002

laser pulse duration; the latter were found to increase with the duration of the switched-out pulse.

A direct interpretation and comparison of the studies in the literature in which different laser pulse durations have been employed is considerably hampered by the differences in the experimental set-ups: Different types of mass spectrometers and modes of operations (e.g., linear versus reflectron systems) and sample preparation techniques were used. Moreover, only a few matrices have been investigated so far.

A systematic comparison over a broad range of pulse durations and matrices obtained on one instrument does therefore seem highly desirable, and was the objective of the present work. Three different IR lasers with laser pulse durations varying from 6 to 185 ns have been employed for this purpose and a wide range of common MALDI matrices investigated.

The solid knowledge of the influence of the laser pulse duration on the various mass spectrometric measures like threshold fluence, resolution, or the extent of fragmentation can provide hints towards instrumental improvements as well as provide a deeper insight into the processes of desorption and ionization in IR-MALDI.

The variation of the pulse duration between a few nanoseconds and about hundred nanoseconds as realized in this work is of special interest as it spans (for typical IR-MALDI conditions) the transition from simultaneous thermal and acoustic confinement conditions (no significant thermal or mechanic energy loss out of the excited volume during the laser pulse) to the regime of solely thermal confinement. In the latter case, where the depth of the absorption volume (laser penetration depth) is on the same order or larger then the distance stress waves traverse in the time window of the laser pulse duration, a significant built-up of pressure can occur and add to the disintegration of the condensed phase. The results of such experiments should therefore allow for a direct comparison to predictions of desorption models and molecular dynamic (MD) simulations [19]. The results with the short OPO pulse duration of 6 ns can, finally, also be directly compared to related experiments in UV-MALDI in which comparable pulse durations have been employed [20, 21]. Because of the significantly lower penetration depth thermal but no stress confinement is effective under UV-MALDI conditions.

Experimental

Mass Spectrometer

All experiments were carried out with an in-house built single-stage reflectron time-of-flight (REF-TOF) mass spectrometer of 3.5 m equivalent flight length. For the determination of threshold fluences the mass spectrometer was operated in the linear TOF mode (LIN-TOF) with a flight length of 2.16 m. In one experiment for the investigation of the desorption/ion emission time duration a short flight length of 0.18 m was used. The REF-TOF mode was used in some experiments to estimate the extent of metastable decay.

All experiments were carried out in the positive ion mode. Ions were accelerated through a total potential difference of 16–25 kV in a two stage grid Wiley/McLaren ion extraction source with distances S_1 and S_2 of 6 mm and 12.5 mm, respectively. Delayed extraction could be used with a minimum delay time of 120 ns and a maximum switched voltage of 6 kV. Venetian-blind secondary electron multipliers (SEM) (9643/A, Emi-Thorn, Ruislip, UK), equipped with a conversion dynode mounted 10 mm in front of the first dynode of the SEM, were used as standard detectors for ion detection. For analytes exceeding 10 kDa the potential between the conversion dynode and the SEM was set to approximately −15 kV in order to increase the ion signal by efficient detection of secondary ions, produced at the conversion dynode. For the experiments investigating the mass resolution under delayed extraction (DE) conditions a microsphere plate (El-Mul Technologies Ltd., Yavne, Israel) mounted on an impedance-matched anode with a time resolution of about 1.5 ns was used. Signals were processed by a transient recorder (LeCroy 9350A, Chestnut Ridge, NY) with a maximum time resolution of 500 ps and the digitized data transferred to a PC for storage and further evaluation. Samples were observed with a CCD camera at a resolution of about 20 μm.

Laser and Laser Optics

An OPO laser system (Mirage 3000B, Continuum, Santa Clara, CA) pumped by the fundamental and second harmonic of a Nd:YAG laser (Surelite II-10, Continuum) served as wavelength-tuneable short-pulse laser system. The OPO system and the applied optics for beam separation and laser beam steering have been described in detail previously [14]. The OPO generates a 1.45–2.12 μm signal and a 2.12–4.0 μm idler wave in a two stage non-linear parametric process. Wavelength tuning was achieved by computer controlled angle phase matching of the potassium titanyl phosphate (KTP) non-linear crystals. Wavelength calibration was carried out with narrow band filters (Infrared Engineering, Maldon, UK) at 2.40, 3.00, and 3.40 μm. Separation of signal and idler waves was achieved by means of a germanium filter. The bandwidth of the OPO laser is specified by the manufacturer to approximately 10 nm at a wavelength of 3.0 μm. Only the two wavelengths of 2.79 μm (corresponding to the emission wavelength of the Er:YSGG laser) and 2.94 μm (Er:YAG laser) were applied in this study. The shot-to-shot pulse energy stability of the OPO laser at these wavelengths was measured with a high precision energy meter and found to be about $\pm$2%.

The solid-state Er:YSGG laser (SEO 1-2-3, Schwartz Electro Optics, Orlando, FL) was modified by placing a $LiNbO_3$ Pockels cell (Gsänger Optoelektronik, München, Germany) into the resonator beam path. In this Q-switch mode the laser emits 70–80 ns long

pulses. The energy stability for successive laser pulses was about ±3%.

The Er:YAG laser (Speser, Spektrum Laser, Berlin, Germany) was supplied with a $LiNbO_3$ Pockels cell by the manufacturer. Variation of the delay between flash tube discharge and the electro-optical switch permitted adjustment of the laser pulse duration between approximately 90 and 185 ns. Throughout this study two fixed pulse durations of approximately 100 and 185 ns were used. The shot-to-shot energy stability of this laser was about ±5–10% for 100 ns long and ±15% for the 185 ns pulses.

The temporal profiles of the laser pulses were measured with a fast IR-sensitive HgCdTe-detector (Radec Infrared-Detector R004-0, Boston Electronics Co, Brooklin, MA) with a time resolution of ca. 1–2 ns. To a good approximation all three lasers were found to have quasi-Gaussian-shaped temporal emission profiles. Temporal and spatial pulse profiles were especially checked for the Er:YAG laser upon change of the pulse duration between 100 and 185 ns. Neither a spontaneous mode locking (conceivable for this kind of solid state laser system) nor a change in spatial profile were observed for any of the employed delay time settings. Any mode locking is probably simply suppressed by the use of a thin etalon as output coupling mirror. Spontaneous mode locking with amplitudes about 3 ns apart has in fact been observed with the same fast IR photo diode on a second Er:YAG laser of identical type, but equipped with a dielectrically coated output coupling mirror, instead of the etalon.

All IR-laser beams were coupled into the mass spectrometer via the same CaF_2 window at an angle of incidence of 45° relative to the target. Rapid switching between the lasers was realized with beam alignment stages mounted on movable precision carriers outside the vacuum. Exact overlap of the laser foci on the target was checked and ensured during all experiments, as described below. Laser desorption energies were adjusted by angle-variation of a dielectric-coated CaF_2 substrate (Laser Optik, Garbsen, Germany) with a computer-controlled stepper-motor.

Laser pulse duration, pulse energy, irradiated area, and laser wavelength were carefully monitored throughout all experiments. Laser pulse energies were measured "off-line" with a high-precision commercial energy-meter (Laser Precision, Yorkville, NY) by placing the energy meter directly into the beam-line, immediately after the determination of the threshold fluences. Laser pulse energies were averaged over 25 consecutive single laser pulses. Transmission losses caused by all optical elements were determined separately and taken into account. The threshold fluence was defined in this study as the lowest laser fluence for which more than 10% of the spectra exhibited an analyte signal-to-noise ratio of at least 3:1, equivalent to the definition in prior studies [14, 16]. For the determination of threshold fluences, typically five separate threshold measurements with different samples were carried out per pulse duration/wavelength combination. From this set of data the mean threshold fluence and standard deviation were calculated.

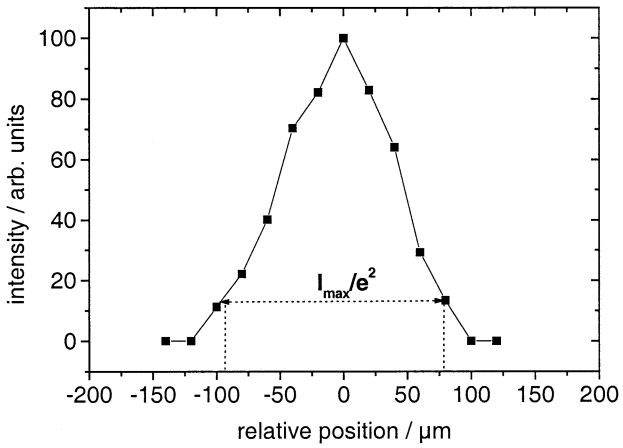

Figure 1. Typical laser beam intensity profile in the focal plane realized for determination of the threshold fluences (see text for further information). The beam profile was recorded by scanning the cross section with a 20 μm wide pinhole and recording the transmitted laser energy.

Control of Irradiation Area

Identical geometrical irradiation conditions were ascertained for all lasers. This is important, because any undetected variation of the size of the irradiated area for different pulse durations (i.e., different laser systems) would induce a corresponding error in the threshold fluence determination. The problem is aggravated by the recent observation of a strong dependence of the threshold fluence on the size of the irradiated area [22].

To achieve a well-defined focal diameter on the sample a pinhole with an aperture of 150 μm in diameter was placed in the focal plane of a CaF_2 lens of 200 mm focal length. With the diameter of 150 μm of the pinhole, significantly smaller than the focuses of all three lasers, only the central part of the three laser beams was transmitted through the pinhole. The pinhole aperture was imaged 1:1 onto the target by two CaF_2 lenses of 100 mm focal length in infinite conjugation. The intensity profile of the laser spots on the target was measured by scanning the beam cross section with a pinhole of 20 μm diameter and recording of the transmitted energy with a high-precision energy meter. A typical profile, as found for all three lasers, is depicted in Figure 1. For a rapid check of the spot size during experiments, burn patterns on photographic paper mounted on the target were used as described elsewhere [14]. The irradiated area was elliptical (as a result of the angle of incidence of the laser of 45°), with a size of $(14.7 \pm 0.9) \times 10^{-9}$ m^2 in the experimental series comparing the Er:YSGG with the OPO laser and $(16.3 \pm 1.0) \times 10^{-9}$ m^2 in the comparison between the Er:YAG and the OPO laser.

Table 1. Threshold fluences for desorption of cytochrome *C* ions from different matrices at a wavelength of $\lambda = 2.94$ μm and three laser pulse durations of $\tau = 6$ ns (OPO laser), $\tau = 98$ ns (Er:YAG laser), and $\tau = 185$ ns (Er:YAG laser)

Laser pulse duration/ns	Threshold fluence/J m^{-2}					
	Succinic acid	DHBs	Phloroglucinol	Thiourea	Glycerol	Triethanolamine
6 ± 0.5	3020 ± 600	1930 ± 110	2570 ± 380	1740 ± 260	3550 ± 180	8810 ± 520
98 ± 4	3650 ± 480	3690 ± 490	4100 ± 520	2910 ± 150	4230 ± 190	10280 ± 560
185 ± 15	3890 ± 480	3530 ± 430	4440 ± 420	2880 ± 350	4190 ± 330	10820 ± 600

For the experiments on the influence of the laser pulse duration on the temporal width of ion signals (ion generation times) and those on the metastable fragmentation, the size of the irradiated area is less critical. These experiments were, therefore, performed by focusing the laser directly onto the target with a single lens. The comparability of the focal diameter for the different lasers was monitored by the burn-pattern method.

Sample Preparation

Succinic acid and thiourea were dissolved in H_2O to concentrations of 20–30 g/l. Phloroglucinol and caffeic acid were dissolved to a concentration of 20 g/l in a 1:1 mixture of water and ethanol. DHBs was prepared as a 9:1 (vol:vol) mixture of 2,5-dihydroxybenzoic and 2-hydroxy-5-methoxybenzoic acid. Unless specifically noted, solid matrix samples were prepared by the standard dried droplet method mixing 1 μl of a 10^{-4} M aqueous solution of cytochrome *C* (horse heart) with 2 μl of the matrix solution followed by drying in a stream of cold air. Liquid matrix samples of glycerol and triethanolamine were prepared on-target by thoroughly mixing the neat matrix liquids with the aqueous analyte solution in a 1 : 1 volume ratio. Prior to insertion of the samples into the high vacuum of the sample chamber, most of the water solvent was rapidly evaporated at a pressure of ca. 10^{-2} mbar in the transfer lock of the mass spectrometer. All chemicals were purchased from Sigma Chemical Co. (Deisenhoven, Germany) or Fluka Chemie AG (Buchs, Switzerland) and used without further purification.

Results

Threshold Fluences

Tables 1 and 2 list the threshold fluences for the desorption of cytochrome *C* ions from various matrices as a function of laser pulse duration for the two wavelengths of 2.94 μm and 2.79 μm, respectively.

The experiments with the Er:YAG laser wavelength at 2.94 μm revealed a clear trend (Table 1). For all matrices lower mean threshold fluences, H_0, were found for the short OPO laser pulse. The most pronounced differences were found for DHBs (decrease in H_0 by a factor of 1.9), and phloroglucinol and thiourea (decrease in H_0 by a factor of 1.7). For succinic acid, glycerol, and triethanolamine a less strong but still significant reduction by a factor of about 1.2 was found. Increase in pulse duration of the Er:YAG laser from ca. 100 to 185 ns was, however, not accompanied by a statistically significant further change in threshold fluence for any of the compounds.

For the Er:YSGG laser wavelength a decrease in threshold fluence of about a factor of 1.7 was found for caffeic acid by switching from 75 to 6 ns (Table 2). Caffeic acid shows a very good mass spectrometric performance at the 2.79 μm wavelength [14] and was used therefore as a substitute for thiourea (Table 1), which does not yield mass spectra at the Er:YSGG wavelength. Succinic acid and DHBs showed a decrease in threshold fluence of about a factor of 1.2–1.3 for the shorter pulse duration. Within the error margins no significant change in threshold fluence upon the variation of pulse durations at the 2.79 μm wavelength was found for solid phloroglucinol as well as for the liquid matrices glycerol and triethanolamine.

Ion Formation Times

The experiments described in this and the subsequent two sections were performed to probe for a potential influence of the laser pulse length on the duration of the desorption/ionization event, the initial kinetic energy distribution, and the metastable ion decay. Only the Er:YAG wavelength of 2.94 μm and succinic acid and glycerol, representative for solid and liquid state IR-MALDI matrices were used.

To test the influence of the laser pulse duration on the time frame of desorption/ionization, a set-up with a

Table 2. Threshold fluences for desorption of cytochrome *C* ions from different matrices at a wavelength of $\lambda = 2.79$ μm and two laser pulse durations of $\tau = 6$ ns (OPO laser) and $\tau = 75$ ns (Er:YSGG laser)

Laser pulse duration/ns	Threshold fluence/J m^{-2}					
	Succinic acid	DHBs	Phloroglucinol	Caffeic acid	Glycerol	Triethanolamine
6 ± 0.5	8970 ± 1010	4280 ± 660	4010 ± 270	2380 ± 230	5880 ± 710	13760 ± 1530
75 ± 2	11440 ± 630	5000 ± 310	4190 ± 310	4030 ± 300	5340 ± 380	12300 ± 740

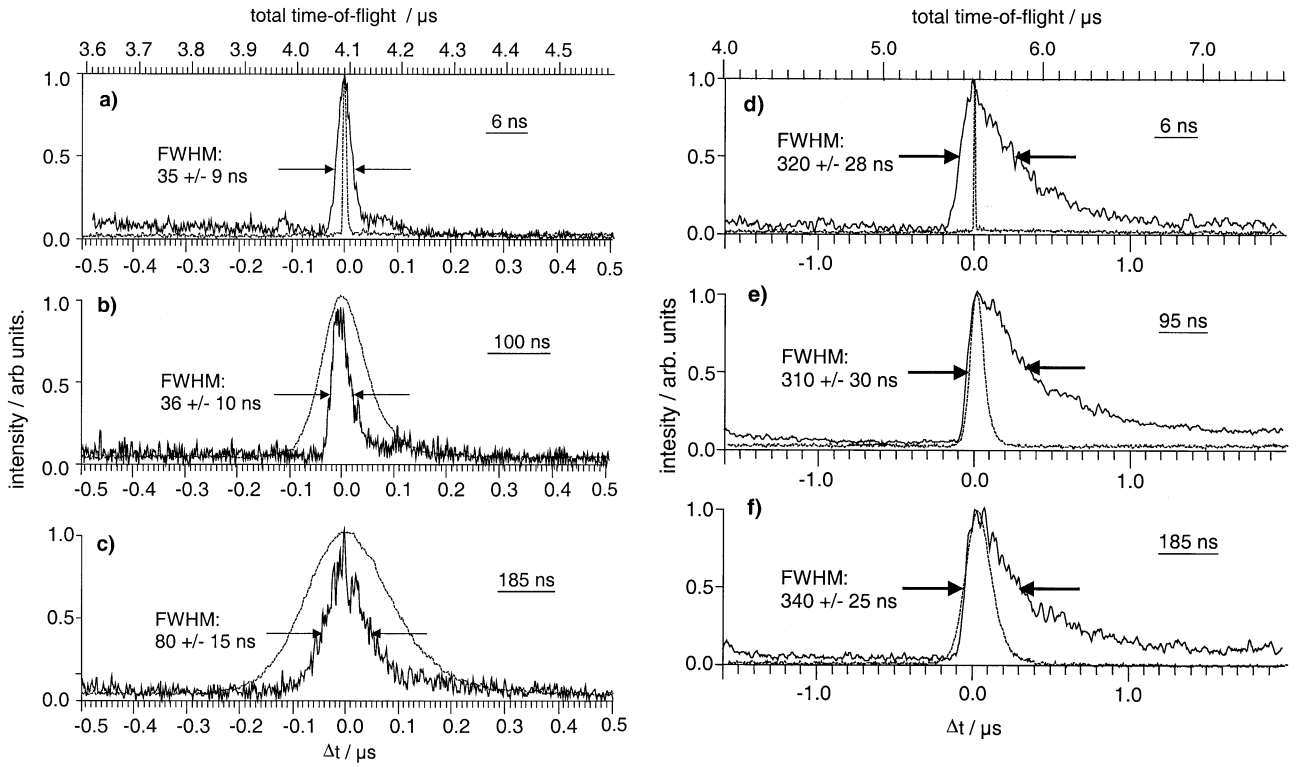

Figure 2. Flight time dispersion of angiotensin I ions (human, 1296.5 Da) as a function of the laser pulse duration τ at a wavelength of $\lambda = 2.94$ μm. (**a**), (**b**), and (**c**), desorbed from a succinic acid matrix: (**a**) $\tau = 6$ ns; (**b**) $\tau = 100$ ns; (**c**) $\tau = 185$ ns. (**d**), (**e**), and (**f**), desorbed from a glycerol matrix: (**d**) $\tau = 6$ ns; (**e**) $\tau = 100$ ns; (**f**) $\tau = 185$ ns. All spectra were recorded with a short field-free drift length of L = 0.18 m and under continuous ion extraction conditions; voltages applied for the first and second acceleration region, S_1, and S_2, respectively, were: $U_{S1} = 2$ kV, $U_{S2} = 23$ kV for (**a**), (**b**), (**c**) and $U_{S1} = 1$ kV, $U_{S2} = 24$ kV for (**d**), (**e**), (**f**). Each spectrum represents the sum of five [(**a**), (**b**), (**c**)] or twenty [(**d**), (**e**), (**f**)] single-shot mass spectra, respectively. For comparison, the temporal profiles of the laser pulses are also plotted (dashed lines), centered to the ion signal.

very short field-free drift length of 0.18 m was used in combination with a high total acceleration potential of 25 kV (under continuous ion extraction conditions). This approach minimizes the contribution of the initial velocity distribution to the overall temporal width of the ion signals (flight time dispersion). Figure 2a, b, c display signals of angiotensin I ions desorbed from the succinic acid matrix with three different pulse durations. Whereas almost identical ion signals widths of approximately 35 ns (FWHM) are found for the two laser pulses of 6 and 100 ns, an increase to about 80 ns is seen for the 185 ns pulse.

For glycerol a significantly longer but completely pulse duration independent ion signal width of about 320 ns (FWHM) is found for all three laser pulse durations (Figure 2d, e, f). In addition, a pronounced signal tailing towards longer flight times is observed for this matrix. The slightly longer total flight time in Figure 2d, e, f compared to Figure 2a, b, c results from a lowered extraction field applied in the first stage of the two-stage ion source, as generally favorable for liquid matrices. In part, it can also be attributed to a generally higher energy deficit as reported recently for liquid matrices [23]. To prevent any influence of cation adduct formation the glycerol used in these experiments was purified beforehand with cation exchange beads. Control experiments, applying delayed ion extraction under otherwise identical experimental conditions, which resulted in a time resolution sufficient to resolve alkali cation formation also for the short TOF, indeed proved that the observed tailing is not due to excessive cationization.

Initial Energy Distributions

In contrast to the above procedure, the normal LIN-TOF mode of the instrument with a field-free drift length of 2.16 m but a low overall acceleration potential of 5 kV (continuous ion extraction) was chosen to test the possible influence of the laser pulse duration on the initial energy distribution. Under these conditions the ion signal width is dominated by the dispersion in flight times due to the initial energy distribution, whereas the relative contribution of the ion generation time is minimized. In this mode of comparably long flight times all three laser pulse durations generated almost indistinguishable quasi-Gaussian ion time-of-flight distributions of about 200 ns in width for the succinic acid

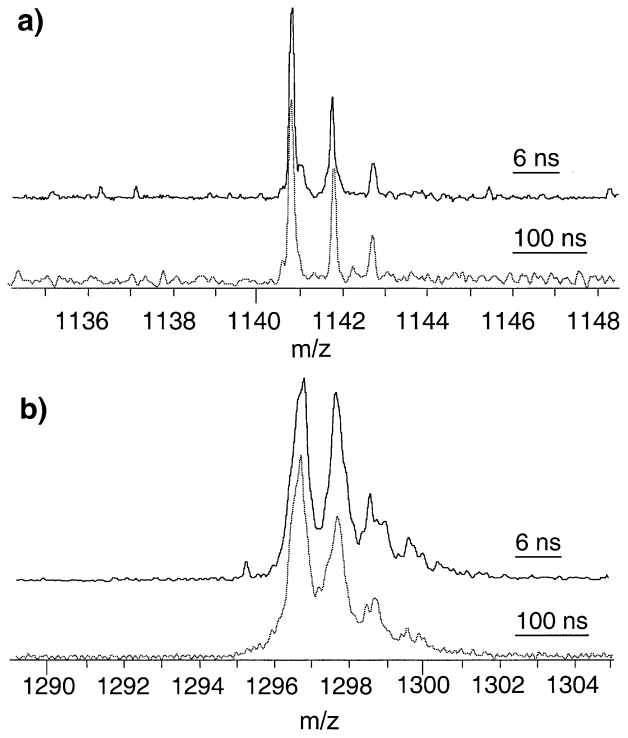

Figure 3. Mass resolution as a function of laser pulse duration under optimized delayed extraction (DE) conditions for laser pulse durations of τ = 6 ns (solid lines, OPO laser, λ = 2.94 μm) and τ = 100 ns (dashed lines, Er:YAG laser, λ = 2.94 μm). (**a**) Signals of gramicidin *S* ions (*Bacillus brevis*, 1140.5 Da) desorbed from a succinic acid matrix. The widths of the signals correspond to a mass resolution m/Δm of about 11.000 (FWHM) for both lasers. Spectra were recorded in the DE-LIN-TOF mode of the mass spectrometer. Each spectrum represents a single-shot mass spectrum. (**b**) Signals of angiotensin I ions (human, 1296.5 Da) desorbed from a glycerol matrix. The widths of the isotopic ion signals correspond to a mass resolution m/Δm of about 3500 (FWHM) for both lasers. Spectra were recorded in the DE-LIN-TOF mode of the mass spectrometer. Each spectrum represents the sum of 20 single-shot mass spectra.

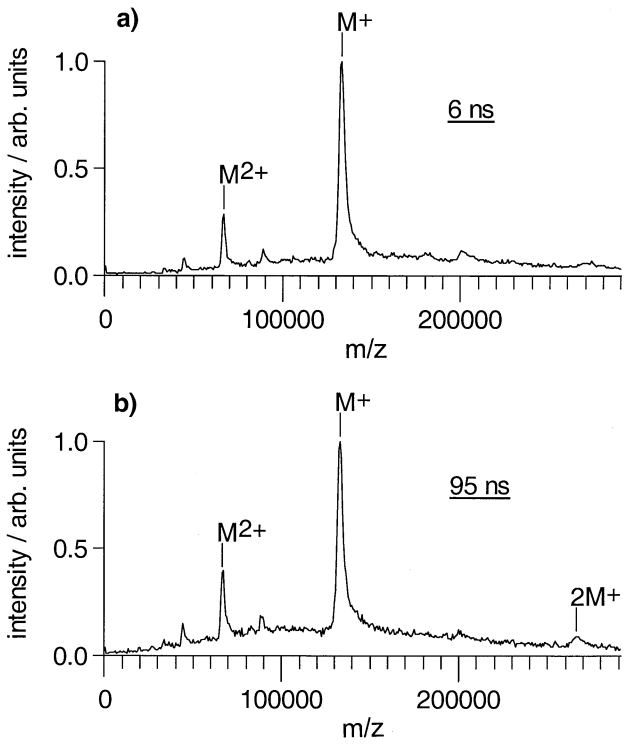

Figure 4. IR-MALDI mass spectra of a 430 mer DNA single-strand molecule desorbed from a glycerol matrix at λ = 2.94 μm with laser pulse durations of (**a**) τ = 6 ns and (**b**) τ = 95 ns. All spectra represent the sum of 15 single-shot mass spectra and were recorded in the REF-TOF mode of the instrument.

matrix (spectra not shown). For glycerol, again, significantly broader ion signal widths of about 1 μs were obtained, also indistinguishable at the three laser pulse durations (spectra not shown). These findings indicate pulse duration independent but strongly matrix dependent distributions of the initial ion kinetic energies.

The influence of the laser pulse duration on the overall ion signal width, i.e., the mass resolution, was also examined under delayed ion extraction (DE) conditions and for laser pulse durations of 6 ns and 100 ns (Figure 3). Despite the distinctly different laser pulse durations, identical signal widths of ~1.5 ns are obtained for the isotopes of gramicidin *S* out of a succinic acid matrix (Figure 3a). The FWHM signal width of 1.5 ns simply reflects the time resolution of the microsphere plate detector employed in this experiment. The achieved maximum mass resolution m/Δm of 11,000 (FWHM) is furthermore equal to the UV-MALDI performance of the same instrument. As for continuous extraction conditions, peptide ion signals are considerably less well resolved if glycerol is used as matrix; a maximum mass resolution of 3500 (FWHM) is achieved in this case (Figure 3b; angiotensin I was used as the test peptide in this case).

Metastable Fragmentation

The potential influence of the laser pulse duration on the extent of metastable fragmentation in IR-MALDI was examined for large labile proteins and nucleic acids (the lack of a post source decay [PSD] option on the employed mass spectrometer did not permit an analysis of the metastable decay of peptides). For large macromolecular compounds, usually, a substantial degradation of the mass spectra due to metastable decay results in a pronounced tailing of the ion signals towards shorter flight times in the REF-TOF mode. Figure 4 shows spectra of a 430 mer single stranded DNA molecule analyzed with a glycerol matrix in the REF-TOF mode (continuous extraction conditions). A peak tailing was not observed for any of the different laser pulse durations. Similar observations were made for large proteins, exceeding ca. 50 kDa, for which a strong metastable decay is commonly found in UV-MALDI (spectra not shown). The generally low degree of metastable fragmentation typical for IR-MALDI [4–9] is hence not laser pulse duration dependent.

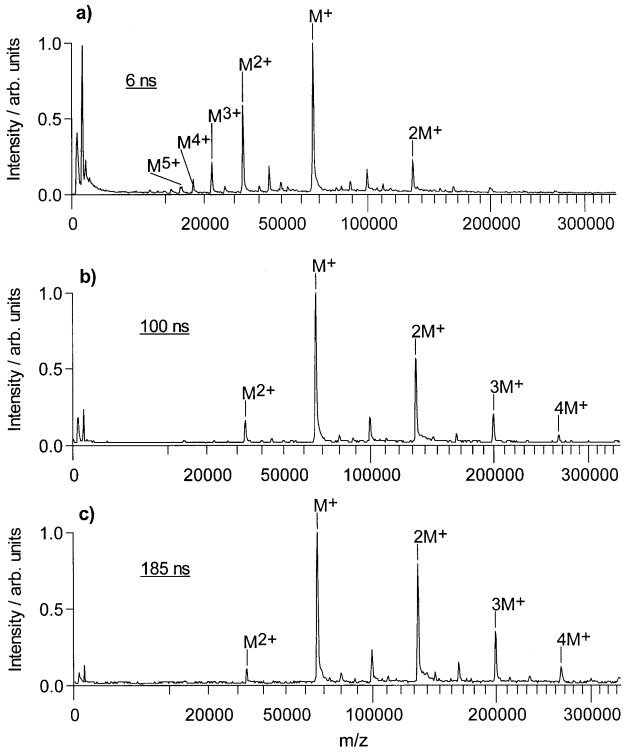

Figure 5. IR-MALDI mass spectra of bovine serum albumin desorbed from a glycerol matrix with laser pulse durations of (**a**) $\tau = 6$ ns, (**b**) $\tau = 100$ ns, and (**c**) $\tau = 185$ ns. All spectra represent the sum of ten single-shot mass spectra and were recorded in the REF-TOF mode of the instrument.

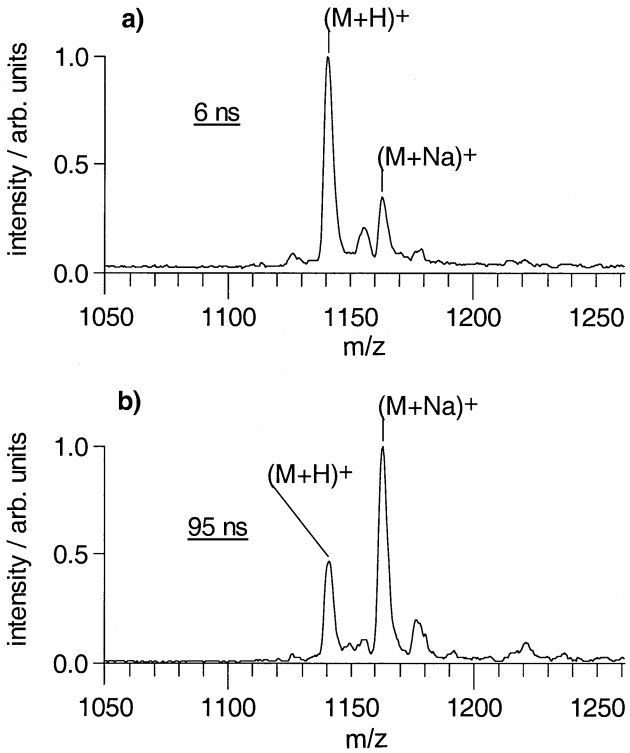

Figure 6. IR-MALDI mass spectra of gramicidin *S* (*Bacillus brevis*) desorbed from a glycerol matrix at $\lambda = 2.94$ μm with laser pulse durations of (**a**) $\tau = 6$ ns and (**b**) $\tau = 95$ ns. Each spectrum represents the sum of 15 single-shot mass spectra. Spectra were recorded in the DE-LIN-TOF mode of the instrument.

Charge State and Oligomer Distributions

With the two exceptions described below, a substantial influence of the laser pulse duration on charge state or oligomer distribution was not observed for any of the tested analyte/matrix combinations; neither were the ratios between protonated and cationized quasimolecular ions signals found to be notably affected.

Two interesting pulse durations effects were, however, detected for the glycerol matrix. The first relates to the analysis of (large) proteins. As an example, three mass spectra of bovine serum albumin (MW, 66.4 kDa) recorded at the Er:YAG wavelength of 2.94 μm and with the three laser pulses of 6, 100, and 185 ns in duration are displayed in Figure 5. Whereas, with the two long Er:YAG laser pulses, a pronounced distribution of BSA oligomers but only few multiply charged BSA ions are generated, this relation reverses for the short OPO pulses under otherwise identical experimental conditions.

The second pulse duration effect was observed for the desorption/ionization of gramicidin *S* from glycerol matrix (Figure 6). A clearly favored generation of alkalicationized gramicidin *S* molecules was found for the two long Er:YAG laser pulses of 95 and 185 ns, whereas the protonated gramicidin *S* signal forms the base peak in the 6 ns OPO spectrum. This peculiar behavior is specific for gramicidin *S*, and most probably, related to its cyclic structure—no comparable effects were observed for linear peptides or proteins.

Discussion

Compared to the ratios in pulse durations of the two Erbium lasers to that of the OPO laser of 12.5, 16, and 31, respectively, the observed reductions in threshold fluences differ "only" by a factor of 1.2 to 1.9. For some matrices even no reduction at all was observed at 2.79 μm and within the error margins. IR-MALDI with lasers emitting in the 3 μm wavelength range and pulse durations in the low nanosecond to 200 ns range, therefore, appears to be essentially determined by the overall amount of deposited energy per unit volume and laser pulse, i.e., by laser fluence rather than by laser irradiance.

The reason for the somewhat different extent in threshold reduction for the individual matrices is not straightforwardly obvious, nor that for the slightly different behavior at the two IR wavelengths. The observed weak dependence of the threshold fluence on the pulse duration is, however, in apparent contrast to results reported previously by Cramer et al. [16, 18]. These authors reported an approximately constant threshold irradiance rather than a constant threshold fluence for wavelengths in the 3 μm region. This difference can tentatively be attributed to the picosec-

ond pulse structure of the FEL laser and/or the different pulse length range of 100 ns to a few μs investigated in the experiments of Cramer et al.

A straightforward reason for the reduced threshold fluences as seen in our study would be relevant energy dissipation during the laser pulse duration. Such loss mechanisms could possibly also explain the observed differences for the different matrices and wavelengths. Using the previously determined laser penetration depths for MALDI relevant fluence conditions [14], thermal relaxation times on the order of microseconds (glycerol) to even milliseconds (succinic acid) are readily calculated. Thermal confinement conditions are hence clearly affective for all tested matrix/wavelength/pulse duration combinations.

A more complex situation is however found if energy loss by stress waves (pressure pulses) is considered. A possibly relevant build-up of pressure can occur if the deposited laser energy remains essentially confined to the excitation volume during the laser pulse duration. This is the case if the time constant for acoustic energy dissipation, τ_{ac}, commonly defined by the ratio of laser penetration depth and velocity of sound in the material, is greater than the laser pulse duration τ. In fact, the laser penetration/laser pulse lengths conditions realized in this study span the critical transition range. For succinic acid, for example, with a particular large laser penetration depth on the order of 100 μm [14], clear stress confinement conditions are fulfilled at the OPO laser pulse width of 6 ns whereas at the 100 ns of the Er:YAG laser a considerable amount of acoustic energy will already dissipate during the laser pulse duration. For glycerol as the other extreme of particularly low laser penetration depth on the order of 2–3 μm at 2.94 μm [14], τ_{ac} follows to 1–1.5 ns. A considerable reduction in peak pressure is therefore already to be expected at the short laser pulse; at 100 ns, photomechanical stress must be assumed to be rather negligible for the overall process.

Ablation by spallation as the result of the build-up of large tensile stress has previously been proposed by Dingus and Scammon [24] and other authors to explain laser-induced solid state disintegration at low-volume energies. Cramer et al. adopted these considerations to explain the mechanisms of IR-MALDI from a succinic acid matrix at the excitation wavelength of 2.94 μm [16]. To account for possible losses for laser pulse durations exceeding the acoustical relaxation time, Dingus and Scammon introduced a damping factor $D = (1 - e^{-\theta})/\theta$ into their model, where $\theta = \tau/\tau_{ac}$ [24]. In terms of a predominantly spallation-driven ablation mechanism for IR-MALDI, a reduction in peak pressure by the application of longer laser pulses would therefore have to be compensated for by experimentally measurable higher threshold fluences.

Adopting the above equation of Dingus and Scammon differences in peak pressure of about an order of magnitude are calculated for the different experimental pulse lengths and the matrix/wavelength conditions of this work: For succinic acid, the 6 ns long pulses are clearly in the stress confined regime (based on the above average value of ~100 μm for the penetration depth at 2.94 μm wavelength [14, 22] and an estimated speed of sound of ~3000 ms^{-1}, τ_{ac} follows to 33 ns), whereas stress confinement conditions are not fulfilled for the longer Er:YAG laser pulses. These differences are clearly not reflected in a corresponding change of the experimental threshold fluences.

Whereas these findings do, therefore, not substantiate the assumption of a predominant spallation mechanism for IR-MALDI from succinic acid, two important aspects have yet to be pointed out. One is that the investigated solid-state matrix preparations do not typically form ideal bulk materials but instead, consist of irregular arrangements of small crystallites with sizes comparable to the laser penetration depths. Reflections at the macroscopic crystal surfaces and at microscopic boundaries in the imperfect crystallites must be assumed to eventually significantly affect pressure wave propagation. The second, perhaps even more important aspect is that only ions were recorded in our study. Optical observation of samples as well as recent photoacoustic studies [25], in which the material ablation of glycerol was recorded as a function of laser fluence, show that effective ablation takes place already at fluences considerably below the ionization threshold. A potential change in ionization efficiencies upon change in laser pulse duration would imply that an interpretation of the ion data with respect to desorption mechanisms were at least problematic. The photoacoustic data [25] indeed suggest that at least for IR-MALDI from glycerol (the only matrix measured in some detail so far) ionization efficiencies are different for the two laser pulse durations of 6 and 100 ns. Further detailed investigations on the material ablation and the ionization efficiencies are however clearly desirable to further elucidate these important issues.

For DHBs and thiourea, having a much stronger absorption at 2.94 μm wavelength [14, 22], the pressure change with pulse duration should even be higher than for succinic acid, which is also in clear contradiction to the experimental findings. These considerations indicate that based on the mass spectrometric ion data, neither a simple spallation model is sufficient to explain the IR-MALDI process of solid state matrices nor would, given the low densities of energy per volume for some matrices, and in particular succinic acid [14, 16, 22], any pure thermal model.

In contrast to the solid state matrix preparations, glycerol is a relatively well defined and homogenous material. The acoustic relaxation times at both wavelengths are already slightly shorter than the duration of the OPO laser pulse (τ_{ac} = 1–2 ns at 2.94 μm). Glycerol is, on the other hand, a relatively strongly absorbing matrix with a decadic molar extinction coefficient of ~175 l mol^{-1} cm^{-1} at 2.94 μm [14]. The energy density in the upper surface volume and at threshold fluence follows to ~100 kJ mol^{-1} [22], close to the heat of

vaporization of this material. For this matrix, rapid thermal heating, therefore, likely forms the basis of the overall process at all three pulse durations. A photomechanical component is likely to add in particular at the short 6 ns excitation. The hereby modified disintegration mechanisms also appear as the likely reason for the observed pulse duration effects on the charge state and oligomer distribution for proteins (Figure 5) and the yield of cationized versus protonated gramicidin *S* molecules (Figure 6).

Recent molecular dynamics simulations by Zhigilei and Garrison have also addressed a comparison of thermal- and stress-confinement. Two excitation pulse durations differing by a factor of ten were applied in this work [19]. These simulations indeed suggest a significant contribution of photoacoustic pressure at stress confinement conditions, though on the background of a predominantly thermal excitation of the volume at both pulse durations. The observed reduction in the "ablation" threshold fluence of about a factor of 1.2 in this computational study, moreover, is in fact on the same order as the experimental values of the present work. A limitation of the MD simulations is at present set however by the current maximum simulations volume of ca. 100 nm in depth.

Our IR-MALDI results can also be compared to previous experimental investigations on the pulse width dependence in UV-MALDI [21]: For the range set by the two nitrogen lasers employed in that study with pulse lengths of 0.5 and 3 ns, both realizing thermal but not stress confinement, threshold fluences were found to be laser pulse duration independent.

The findings from the experiments on the ion formation times (Figure 2) confirm previous observations [16, 18] that desorption/ionization from solid state matrices in IR-MALDI occurs on a time scale significantly shorter than the duration of the 100 ns or longer Er:YAG laser pulses. The longer observed ion generation times for the 185 ns long laser pulse excitation (Figure 2c) might, however, indicate a change in the involved processes for longer laser pulses. A prolongation of ion emission with pulse duration was previously also reported by Cramer et al. [16] in their work with varied macro pulse lengths of the FEL.

The different temporal signal profiles for succinic acid and glycerol in the "time-resolved" measurements with the short TOF-MS point to considerably different desorption/ionization mechanisms for the two matrix classes.

For glycerol, time-of-flight ion profiles were completely independent of the laser pulse duration for both employed field-free drift lengths. It must however be assumed that even with the short TOF possible differences in ion emission times are likely to be concealed by the wide kinetic energy distribution of analyte ions desorbed from this matrix [23]. The equal flight time profiles at the three pulse lengths (Figure 2d, e) can therefore not be taken as ultimate proof for equal ion emission times. Our recent photoacoustic studies on IR-MALDI have indeed shown strong differences for at least the overall material ablation times at 6 and 100 ns laser excitation [25]. Further experiments are necessary to reveal whether these differences also apply to the ion formation times.

The possibly generally longer desorption/ionization times for liquid as for solid state matrices as seen in Figure 2 can, particularly in combination with the broader initial velocity distribution [23], have a pronounced negative effect on the attainable mass resolution under delayed extraction conditions (Figure 3b). A prolonged period of time for the desorption/ionization process will necessarily lead to a considerable space distribution of the ions during the extraction delay time. Hence, the overall resolution will suffer as a simultaneous space and velocity focusing is not possible in a delayed extraction ion source, as has already been pointed out by Wiley and McLaren [26]. The mass resolution of about 3500 (FWHM) as in Figure 3b was the best achievable on our instrument with the glycerol matrix. Recent work by Cramer and Burlingame, however, shows that also from glycerol matrix a temporal resolution, comparable to that of IR-or UV-MALDI from solid state matrices, is possible, if the glycerol drop is placed in a vial in the target, covered with a field defining grid, instead of the plain target surface [27]. The enhanced field-free expansion results in a thinning-out of the plume prior to ion extraction on the one hand, favoring ion extraction with a reduced number of collisions, and the extraction of ions from a small part of the overall expanding plume with a narrower velocity spread on the other.

Conclusions

The influence of the laser pulse duration on the desorption/ionization process in IR-MALDI has been evaluated for laser pulses between 6 and 185 ns in duration. A clear, but if directly compared to the investigated pulse duration range only relatively weak tendency towards reduced threshold fluences with laser pulse length was found for most of the tested matrices at the two examined wavelengths of 2.79 μm and 2.94 μm. The experimental findings raise some doubts on the applicability of a pure spallation model for IR-MALDI, discussed extensively in the literature. Our results rather indicate a combined process of thermal/photomechanically-induced condensed phase disintegration, of which the photomechanical contribution reduces with increasing pulse length, in agreement with recent MD simulations.

The actual contribution of photoacoustic stress in the IR-MALDI process should be investigated in more detail, for example by time resolved measurements with a fast sensitive piezoelectric stress sensor. These experiments are currently under way in the authors' laboratory. Our results also show that the different lasers employed in this study, OPO versus Q-switched

solid state erbium lasers, can be equally well utilized for IR-MALDI.

Acknowledgments

This work was done in partial fulfillment of the requirements for the degree of Dr. rer. nat. of CM at the University of Münster. The authors greatly appreciate financial support by grant no. Hi 285/8-2 of the German National Research Council (DFG) and by grant no. IVA1-800 985 96 of the Department of Education and Research (MWF) of the State of Nordrhein-Westfalen.

References

1. Karas, M.; Hillenkamp, F. *Anal. Chem.* **1988,** *60,* 2299–2301.
2. Overberg, A.; Karas, M.; Bahr, U.; Kaufmann, R.; Hillenkamp, F. *Rapid. Commun. Mass Spectrom.* **1990,** *4,* 293–296.
3. Overberg, A.; Karas, M.; Hillenkamp, F. *Rapid. Commun. Mass Spectrom.* **1991,** *5,* 128–131.
4. Berkenkamp, S.; Menzel, C.; Karas, M.; Hillenkamp, F. *Rapid Commun. Mass Spectrom.* **1997,** *1,* 1399–1406.
5. Siegel, M. M.; Tabei, K.; Kunz, A.; Hollander, I. J.; Hamann, R. P.; Bell, D. H.; Berkenkamp, S.; Hillenkamp, F. *Anal. Chem.* **1997,** *69,* 2716–2726.
6. Niu, S.; Zhang, W.; Chait, B. T. *J. Am. Soc. Mass Spectrom.* **1998,** *9,* 1–7.
7. Cramer, R.; Richter, W. J.; Stimson, E.; Burlingame, A. L. *Anal. Chem.* **1998,** *70,* 4939–4944.
8. Berkenkamp, S.; Kirpekar, F.; Hillenkamp, F. *Science* **1998,** *281,* 260–262.
9. Menzel, C.; Berkenkamp, S.; Hillenkamp, F. *Rapid. Commun. Mass Spectrom.* **1999,** *13,* 26–32.
10. Caldwell, K. L.; McGarity, D. R.; Murray, K. K. *J. Mass Spectrom.* **1997,** *32,* 1374–1377.
11. Sadeghi, M.; Olumee, Z.; Tang, X.; Vertes, A.; Jiang, Z. X.; Henderson, A. J.; Lee, H. S.; Prasad, C. R. *Rapid. Commun. Mass Spectrom.* **1997,** *11,* 393–397.
12. Sheffer, J. D.; Murray, K. K. *Rapid Commun. Mass Spectrom.* **1998,** *12,* 1685–1690.
13. Zhang, W.; Niu, S.; Chait, B. T. *J. Am. Soc. Mass Spectrom.* **1998,** *9,* 879–884.
14. Menzel, C.; Dreisewerd, K.; Berkenkamp, S.; Hillenkamp, F. *Int. J. Mass Spectrom.* **2001,** *207,* 73–96.
15. Cramer, R.; Hillenkamp, F.; Haglund, R. F. *J. Am. Soc. Mass Spectrom.* **1996,** *7,* 1187–1193.
16. Cramer, R.; Haglund, R. F.; Hillenkamp, F. *Int. J. Mass Spectrom. Ion Processes* **1997,** *169/170,* 51–67.
17. Hess, W. P.; Park, H. K.; Yavas, O.; Haglund, R. F. *Appl. Surf. Sci.* **1998,** *127/129,* 235–241.
18. Cramer, R. *Ph.D. thesis*, University of Muenster, 1997, p 18.
19. Zhigilei, L. V.; Garrison, B. J. *J. Appl. Phys.* **2000,** *88,* 1281–1298.
20. Demirev, P.; Westman, A.; Reimann, C. T.; Hakansson, P.; Barofsky, D.; Sundqvist, B. U. R.; Cheng, Y. D.; Seibt, W.; Siegbahn, K. *Rapid Commun. Mass Spectrom.* **1992,** *6,* 187–191.
21. Dreisewerd, K.; Schürenberg, M.; Hillenkamp, F. *Int. J. Mass Spectrom. Ion Processes* **1996,** *154,* 171–178.
22. Feldhaus, D.; Menzel, C.; Berkenkamp, S.; Hillenkamp, F.; Dreisewerd, K. *J. Mass Spectrom.* **2000,** *35,* 1320–1328.
23. Berkenkamp, S.; Menzel, C.; Hillenkamp, F.; Dreisewerd, K. *J. Am. Soc. Mass Spectrom.* **2002,** *13,* 209–220.
24. Dingus, R. S.; Scammon, R. J. in Jacques, S. L. (Ed.), *Laser–Tissue Interaction II, Proc. SPIE Vol. 1427*, 1991, Bellingham, WA, pp 45–54.
25. Menzel, C.; Rohlfing, A.; Berkenkamp, S.; Leisner, A.; Ehring, H.; Kukreja, L. M.; Hillenkamp, F.; Dreisewerd, K. *Proceedings of the 49th ASMS Conference of the American Society of Mass Spectrometry and Allied Topics*, Chicago, IL, May 27–31, 2001, ASMS, Sante Fe, MN, A010050.
26. Wiley, W. C.; McLaren, I. H. *Rev. Sci. Instrum.* **1955,** *26,* 1150.
27. Cramer, R.; Burlingame, A. L. *Rapid Commun. Mass Spectrom.* **2000,** *14,* 53–60.